# Non invasive real time access to spatial attention information from 3T fMRI BOLD signals

***C. Loriette*[1], *C. De Sousa*[1], *S. Clavagnier*[1], *F. Lamberton*[2], *D. Ibarolla*[2], *S. Ben Hamed*[1]**

1. Institut des Sciences Cognitives Marc Jeannerod, CNRS UMR 5229, Université Claude Bernard Lyon 1, 67 Boulevard Pinel, 69675 Bron Cedex, France

2. CERMEP-imagerie du vivant, 59 Boulevard Pinel, 69677 Bron Cedex, France

***Corresponding author:*** Celia Loriette, celia.loriette@isc.cnrs.fr, Suliann Ben Hamed, benhamed@isc.cnrs.fr

***Running title:*** fMRI-based decoding of attention

***Keywords:*** fMRI, decoding, spatial attention, machine learning, single subjects

## Abstract

Access to higher cognitive functions in real-time remains very challenging, because these functions are internally driven and their assessment is based onto indirect measures. In addition, recent finding show that these functions are highly dynamic. Previous studies using intra-cortical recordings in monkeys, succeed to access the (x,y) position of covert spatial attention, in real-time, using classification methods applied to monkey prefrontal multi-unit activity and local field potentials. In contrast, the direct access to attention with non-invasive methods is limited to predicting the attention localisation based on a quadrant classification. Here, we demonstrate the feasibility to track covert spatial attention localization using non-invasive fMRI BOLD signals, with an unprecedented spatial resolution. We further show that the errors produced by the decoder are not randomly distributed but concentrate on the locations neighbouring the cued location and that behavioral errors correlate with weaker decoding performance. Last, we also show that the voxels contributing to the decoder precisely match the visual retinotopic organization of the occipital cortex and that single trial access to attention is limited by the intrinsic dynamics of spatial attention. Taken together, these results open the way to the development of remediation and enhancement neurofeedback protocols targeting the attentional function.

# Introduction

Accessing information generated by the brain in real-time has been a major challenge these past years. Indeed, decoding brain activity in real-time can be used to develop neuroprostheses, or design remediation or brain training protocols using neurofeedback approaches (Loriette and Ziane, 2021). It can also be used to enhance our understanding of the neural and network bases of cognition (Loriette et al., 2021). Thanks to advances in feature detection and machine learning approaches (Abraham et al., 2014), considerable progress has been made in both animal (Astrand et al., 2016; Branco et al., 2017; Brown et al., 1998; Padmanaban et al., 2018; Tremblay et al., 2015) and human research fields (Glaser et al., 2020; Grootswagers et al., 2017; Tong and Pratte, 2012). For example, sensory and motor brain signals can now be decoded with high accuracy using both invasive (Bouton et al., 2016; Branco et al., 2017; Hatsopoulos et al., 2004; Ibayashi et al., 2018) and non-invasive techniques (Kamitani and Tong, 2005; Schwarz et al., 2017; Wen et al., 2018). In the present study, we focus on real-time spatially resolved access to the spatial locus of attention -or attentional spotlight- using BOLD fMRI signal approaching what has recently been achieved using invasive intra-cortical recordings in macaque monkeys (Astrand et al., 2020, 2016; De Sousa et al., 2021; Gaillard et al., 2020).

Visual attention is a cognitive process which allows to select visual stimuli in space for enhanced processing (Boynton, 2005; Gaillard and Ben Hamed, 2020). Spatial attention can be divided in two different processes: overt attention, whereby the eyes move towards the stimulus of interest, and covert attention, which is the process of shifting the focus of attention towards a visual stimulus while the eyes remain stable (Posner, 1980). More precisely, covert attention enhances the detection of the attended stimuli as well as reaction times in response to the stimuli (Carrasco and Yeshurun, 2009). This covert attention is linked to activation of a well-known brain network which includes, in both humans and non-human primates, the frontal eye field (FEF), Intraparietal sulcus (IPS), and the visual cortex (Corbetta et al., 2008; Corbetta and Shulman, 2002; Ibos et al., 2013; Simpson et al., 2011).

While the neural and network bases of covert attention are increasingly understood, accessing this cognitive function in real-time has remained challenging for multiple reasons. One reason for this is the fact that the precise informational content of covert functions can only be assessed indirectly from differed behavioral responses. Another reason pertains to the fact that recent accounts indicate that spatial attention, rather than being stable in space, is actually rhythmic, moving from one spatial location to another (Fiebelkorn et al., 2013; Gaillard et al., 2020; Gaillard and Ben Hamed, 2020; Landau and Fries, 2012). Several studies have been conducted in order to access covert visual attention in real-time. Decoding the (x,y) location of attentional locus has been achieved using intra-cortical electrophysiological recordings in non-human primates (Astrand et al., 2020, 2016; De Sousa et al., 2021; Gaillard et al., 2020). This real-time access to spatial attention is demonstrated to be highly predictive of overt perception and is characterized both by a high temporal (Gaillard et al., 2020) and a high spatial resolution (Di Bello et al., 2021). High decoding performances have also been demonstrated using EEG-based event related responses (ERP) (Thiery et al., 2016). However, this approach is incompatible with single trial level decoding as it depends on the modulation of the response of a visual stimulus by attention and requires an accumulation of data over a numerous number of trials. As a result, accessing the attentional spotlight in real-time using non-invasive techniques in humans remains challenging (Astrand et al., 2014). The decoding of attentional position from EEG recordings currently allows a classification in 2 positions (left and right) with an average decoding performance of 62.6% (Trachel et al., 2015). Classification from fMRI signals achieves 70 to 80% accuracy for 4 quadrant classification (Andersson et al., 2012; Ekanayake et al., 2018). However, in these latter studies, eye movements have not been controlled for. This leads to ambiguous results as it remains difficult to prove that achieved spatial attention decoding is not partly due to eyes movement signals. Moreover, the more recent study uses very high salience visual stimuli in order to guide participant's covert attention, which might also have introduced confounding visual signals to the attentional signals.

In the present study, we aimed to develop an fMRI based, real time method to decode the locus of covert attention in space in humans with an unprecedented high spatial resolution. Specifically, we build a participant specific preprocessing and decoding method which can be deployed in real-time, while subjects are performing an attentional task. To do so, we designed a cued target detection attentional task with very low salience visual stimuli so as to maximize spatial attention processes. This task allows us to achieve reliable decoding at the single trial level. For any given subject, this decoding is reproducible and remains stable across sessions recorded several days apart. Our analyses further show that the errors produced by the decoder are not randomly distributed over all the possible spatial locations but are mainly concentrated on the locations neighbouring the cued location, indicating that classification errors are either due to noise in the signal or, to the fact that attention is intrinsically dynamic, as demonstrated by invasive approaches with non-human primates (Gaillard et al., 2020). Moreover, we show that decoding performance varies as a function of the subjects' attentional behaviour, thus linking attentional engagement in the task to decoding performance. We also show that the voxels contributing to the decoder precisely match the visual retinotopic organization of the occipital cortex (Kastner et al., 1998; Warnking, 2002). These results show that our decoder has been able to target specific attentional regions at the single subject level, at the single trial level. Last, we address the reproducibility of these results and generalize our observations to a similar task based on a different spatial configuration, thus demonstrating the reliability of our method. Taken together, this study demonstrates that we can capture stable covert spatial attentional information at the single trial level using non-invasive fMRI-based brain activity and that these single trial estimates are predictive of overt behavioural performance. These results open the way to the development of remediation and enhancement neurofeedback protocols targeting the attentional function.

# Materials and Methods

## *Participants*

10 participants (4 females, 2 left handed, mean age: 27.22 years, standard deviation: 7.13 years) participated in the experiment. The experimental procedures were approved by the French Ethic Committee (Comité de protection des personnes, #2018-72, ID RCB: 2017-A03612-51), and complied with the declaration of Helsinski. Written informed consent was obtained from all subjects.

## *Experimental setup*

Octave and the Psychophysics Toolbox (Brainard, 1997; Kleiner et al., 2007; Pelli, 1997) were used to generate the visual stimuli and control the experimental procedure within the scanner environment. The visual stimuli were back projected on a screen outside of the bore at a viewing distance of 130 cm and subjects were able to see the display through a mirror placed in front of their eyes. Subjects, lying in the scanner, were instructed to maintain their gaze fixated on a black cross located at the center of the screen against a gray background. Monocular right eye movements of the participants were recorded during scanning process with an EyeLink 1000 fMRI-compatible eye tracker (SR-Research) sampling at 1000 Hz. Eye calibration was performed before each functional scan. Trials were interrupted if the eyes moved outside the 2°x2° eye control window. Interrupted trials were canceled and re-played at the end of the block.

## *Behavioral tasks*

Participants were asked to perform a spatially cued target detection task during which they should fixate a central cross all throughout the trial (0.5°x0.5° of visual angle). After an initial fixation time randomly chosen between 1.5 and 2.5 seconds, a cue (a central black arrow pointing to one of the possible target locations, 1°x1° of visual angle) was presented for 200ms. Participants were explicitly asked to maintain their attention at the cued location. Six to 9 seconds from cue onset, two consecutive targets (a low contrast gray rectangle oriented either vertically -0.5°x1° of visual angle or horizontally -1°x0.5° of visual angle) were

presented for 200ms each and were separated by 150ms (Figure 1A). They had to report if the two targets had the same orientation or not by choosing between two push buttons on a joystick placed in their right hand. Response time was limited to 1 sec after first target onset. Catch trials (i.e. trials with no targets presented) were randomly played and participants had to withhold from any button press. At the end of each trial, a green cross indicated success in the trial, and a red cross indicated error in the trial. Every 5 trials, the participants were asked to maintain their fixation without any attention during 10 seconds. This served as a fixation baseline for the analyses. 5 blocks of 24 trials were performed (3 trials per cue location, presented in a randomized order) per session. Each block lasted about 10 minutes. Prior to each scanning session, the size of the targets was calibrated to reach a 70% of correct responses, using a staircase target detection procedure lasting 60 trials. Two versions of the task were used. Each subject performed 4 sessions of the first behavioral task (3 participants performed 1 session per week during 4 weeks, 1 performed 4 sessions in one week and 6 performed 2 sessions per week during 2 weeks). Four subjects performed 4 sessions of the second version of the task. *Task 1: 8 polar positions and one eccentricity.* Targets could appear at one amongst eight possible spatial locations organized along a circle at an eccentricity of 5°, on the vertical and horizontal meridians as well as on the diagonals. Cues consisted in centrally presented arrows pointing in the expected position of the targets. To help the subjects to correctly hold their attention on the cued location, 8 different locations, corresponding to the 8 different orientations were materialized by a small blank in a white circle at 5° of eccentricity from the center of the screen (Figure 1A). *Task 2: 4 polar positions and two eccentricities.* Targets could be presented at two different eccentricities (5° or 8°) and four different orientations along the diagonals (figure 1A). Cues consisted in centrally presented arrows pointing in the expected position of the targets. Short (1°x1° of visual angle) arrow cues indicated the target would appear on the inner circle while long (1°x1° of visual angle) arrow cues indicated the target would appear on the outer circle.

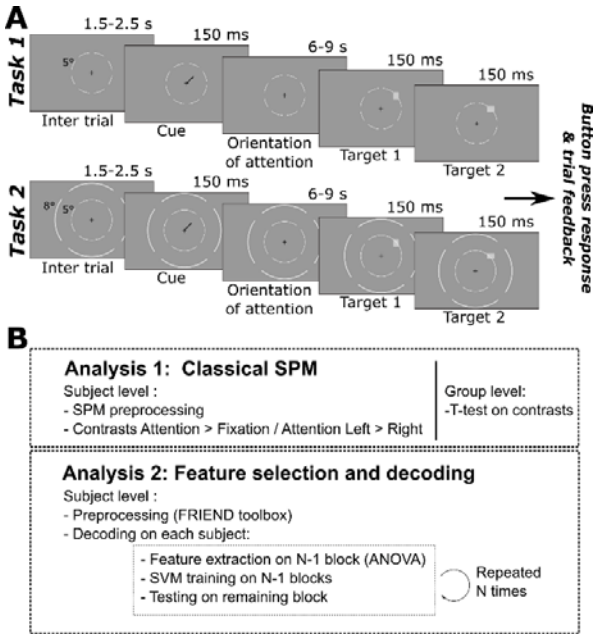


**Figure 1: Behavioral task and analysis pipeline.** A) Spatially cued target detection task. Subjects were required to fixate a central cross all throughout the trial. After an initial fixation time (1.5 to 2.5 s), a cue (a central black arrow pointing to expected target location) was presented for 200ms. Six to 9 seconds from cue onset, two consecutive targets (a gray rectangle oriented either vertically or horizontally) were presented for 200ms each and were separated by 150ms. Subjects had to report target similarity by a button press. Correct trials were followed by a green cross, error trials by a red cross. Two versions of the task were used. Task1: Targets could appear at one amongst eight possible spatial locations organized along a circle at an eccentricity of 5°, on the vertical and horizontal meridians as well as on the diagonals. Task 2: Targets could be presented at two different eccentricities (5° or 8°) and four different orientations along the diagonals. B) Overview of group (Analysis) and single trial decoding (Analysis 2) pipelines.

## *fMRI scanning procedure*

Neuroimaging data were acquired with a 3T MRI scanner (Siemens Prisma) using a 64-channel head coil. Subjects were lying on their back with their head restrained using foam head rest. A High-resolution T1 structural image (MPRAGE, 0.875mm$^3$ isotropic voxels, 192 slices, TR/TE =3.5/3.42s, flip angle, 8°) was acquired during the first session. Functional images were acquired using a multislice T2*-weighted gradient-echo, echo-planar imaging sequence (TR/TE =2200/30ms; flip angle, 90°; 3mm isotropic voxels, 40 interleaved ascending slices with no gap) with a 74x74 acquisition matrix and a 518x518 mm rectangular field of view.

## *Preprocessing for standard event-related analyses*

Preprocessing of the MRI data was performed with Statistical Parametric Mapping software (SPM12; Wellcome Department of Cognitive Neurology, University College London, London, UK; http://www.fil.ion.ucl.ac.uk/spm). The first five volumes of each run were excluded to remove T1 equilibrium effects. Next, within each session, we realigned all successive images to the first image of the session. Slice-timing correction was applied with the time centre of the volume as reference. The subject-mean functional images were co-registered with the corresponding structural images. Functional and structural images were then spatially normalized into standard MNI space. Finally, functional images were smoothed using a 5-mm full-width half-maximum Gaussian kernel. The realignment parameters and the eye movements were used as covariates in subsequent statistical analyses. In order to explore the activations elicited by the orientation of spatial attention, a generalized linear model was designed, by calculating the beta values of the activity elicited by attention orientation to expected targets on the right of the screen, on the left of the screen, or activation observed during fixation. These activations were then contrasted as follows: Attention Right Vs Fixation and Attention Left Vs Fixation. Eye and head movements were used as variables of non interest. Significant T-values ($p<0.05$, FEW-corrected) derived from these contrasts were then displayed on the standard MNI brain.

## *Decoding pre-processing procedure*

For the decoding, and all the following analyses, the functional images were processed in real time using the FRIEND toolbox (the institut d'Or, Brazil) (Basilio et al., 2015; Sato et al., 2013). This allowed a simplified version of preprocessing pipeline. During the acquisition the functional images were transformed in the NIFTI format with the dicom2nii toolbox (Li et al., 2016) and realigned to one reference anatomical image using FSL tools (Jenkinson et al., 2012). No smoothing was implemented as we wanted to keep each vowel as an independent feature. Voxel activity was extracted for each trial and normalized by its mean activity recorded during the fixation period preceding the trial. Prior to decoding, voxels of

interest were chosen based on an ANOVA, testing the significance of the activity of each voxel to one or several of the cued locations during the cue to target interval. Only the significant voxels ($p<0.05$) were selected for decoding using the python neuroimaging toolbox Nilearn (Abraham et al., 2014).

## *Decoding procedure*

A linear SVM (one versus all) was trained on the voxels selected at the decoding preprocessing stage, associating voxel activity patterns to the corresponding spatial cueing condition. Voxel selection and training was performed on all runs except one and trials were balanced in order to have the same number of training trials per position. Testing was then performed on the remaining run, on trials which have thus not been used in for training. This train-test procedure was repeated for each run and a mean decoding performance was then calculated. For the main decoding experiment, this procedure was repeated for each volume from 2.2 seconds before cue onset until 6.6 seconds after target onset. Decoding procedure was performed using the statistical and machine learning toolbox of Matlab (Figure 1B).

## *Statistics analyses*

A permutation test allows to define the chance level and the associated 95% confidence interval of the decoder. All statistical analyses were based on non-parametric tests: Friedman test for paired two way analyses of variance and Kruskall-Wallis for paired one-way analysis of variance. Wilcoxon signed ranked test were used for ad hoc tests on non-independent data. All the statistics were performed using Matlab.

## *Surface and topography analysis*

Brain surfaces and flatmaps were reconstructed via the recon-all pipeline of FreeSurfer 6.0 (Fischl, 2012).

# Results

In this study, our goal was to assess the feasibility of real-time decoding of spatial attention from fMRI BOLD signal and characterize the stability of this decoding in time, within and across sessions. We thus had subjects perform a spatial attention centrally cued target detection task while their brain activity was scanned using a 3T MRI scanner. Attention could be cued towards one out of 8 possible spatial position (Figure 1). Subjects sat in four scanning sessions. In each session they performed 5 blocks of 24 trials per block (performance: Task 1: median=72.2%; s.e.=0.616; Task 2: median=71.1%; s.e.=0.512). Group-level whole brain spatial attention-related brain activation patterns reproduce prior observations (Figure 1A, supplementary note 1 and Figure S1, (Corbetta et al., 2008; Corbetta and Shulman, 2002; Simpson et al., 2011). In the following, we describe single trial decoding of spatial attention orientation (Figure 1B).

## *Single trial decoding of the locus of spatial attention*

The GLM analysis presented in supplementary note 1 identified the voxels that are modulated either by attention, irrespective of spatial position (attention vs. fixation contrast), or by attention to the left vs. attention to the right, irrespective to the precise spatial location attention was cued to. We reasoned that the decoding of spatial attention location from single trial fMRI data will rely on voxels in which activation varies between fixation and attention cued to one or two specific spatial locations. We thus normalized the raw activity of each voxel in the gray matter in time by its raw activity during fixation task epochs. We did not convolve BOLD activity with HRF, so as to remain as close as possible to the recorded signal. We then performed an ANOVA in order to identify the voxels significantly modulated by the position of attention; irrespective of the spatial attention condition it was activated it. This analysis was performed for each subject independently. As we did not convolve the activity with the standard HRF, a 4 to 5 seconds delay is expected between the cue onset and the cue related activations. Activations from 6 seconds from cue onset to target onset was thus taken as attention orientation activations. During this latter interval, strong

activations are observed in the parietal and visual cortex ($p<0.05$, non-corrected) for every single subject (Figure 2, top panel, representative subject). In comparison, when a similar analysis is run at estimated target related activations, 4.4 seconds after target onset, thus indexing visual target perception, reduced activations are observed in the parietal cortex combined with increased activations in the visual cortex (Figure 2, bottom panel, representative subject). These observations are replicated in all individual subjects, and both task versions (data not shown). These voxels were subsequently used to train a decoder.

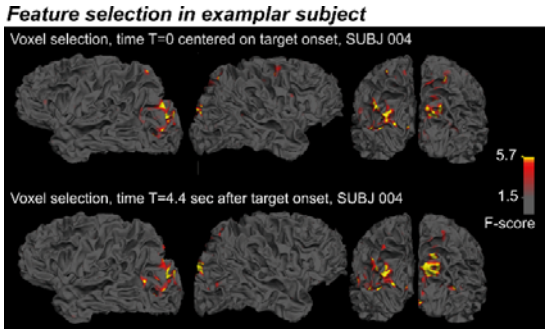


**Figure 2:** Feature selection of attention-related voxels on representative subject: voxels are selected according based on brain volume recorded before target onset (attention, upper panel) and 4.4 sec after target onset (target detection, bottom panel).

For each subject we performed an ANOVA with the position of the cued location as factor, on the volumes from 8.8 secs before target onset to 6.6 secs after target presentation. We then used the significant voxels obtain at each time sample to train and test a linear support vector machine (SVM, one versus all, linear kernel) decoder in order to determine the location of the attentional spotlight. This analysis was performed using a one vs n-1 cross-validation across blocks (feature selection and training were being performed on N-1 blocks, testing was being performed on the remaining block, this procedure being repeated over all possible combinations, Figure 1B). Figure 3A shows the mean decoding performance in time for each subject (grey lines) and averaged over all subjects (Figure 3A, red line, mean +/- s.e.). We observe a significant increase in decoding performance (absolute chance level at 12.5%, dashed lines, the 95% confidence interval calculated with a permutation test in gray) from 4.4 sec after cue onset up to 4.4 seconds after target onset. Decoding performance increases until a plateau is reached between 6.6 seconds after cue onset and 2.2 seconds

after target onset. The mean decoding performance at this plateau is around 40% and can reach up to 58% for some subjects. This plateau is followed by a slight increase in the decoding performance at 4.4 sec after target onset. This observation is reproduced for Task 2 (supplementary figure S2A). On catch trials, i.e. trials in which the target was not presented, decoding performance is undistinguishable from that obtained on target trials, expect for the slight increase in decoding performance at 4.4 secs observed on target trials which is absent in catch trials (Figure3A, blue line, Friedmann: $p<0.05$ for main effects, and signed rank test with $p<0.05$ for ad hoc tests). Thus, the plateau is taken as pure covert attention orientation decoding performance, while the peak observed at 4.4 secs post-target on target trials is taken as a signature of target perception. Taken together, these results show that we can decode covert spatial attention by up to 58% in 8 different locations. This covert attentional information can be differentiated in time from the visual perception response component to target onset.

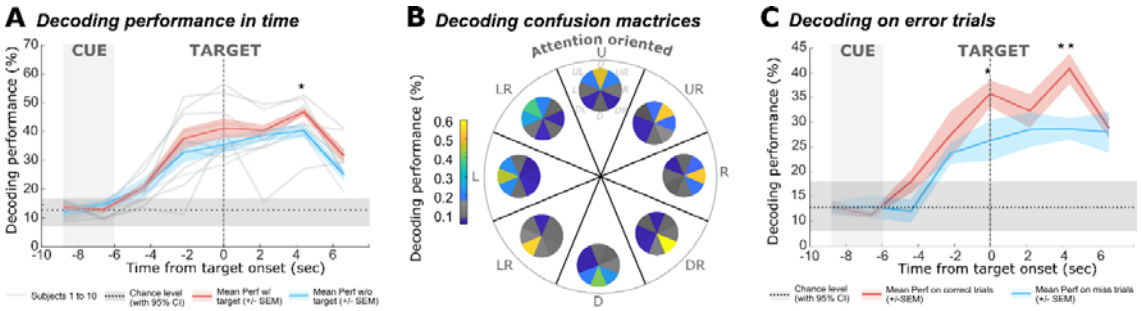


**Figure 3: Linear SVM decoder applied to selected feature modulated voxels allows access to attentional spotlight location with a high accuracy. A.** Decoding performance in time on target present trials (red line, mean+/- s.e.m) or target absent or catch trials (blue line, mean+/- s.e.m). **B.** Confusion matrices per expected target position (smaller pie chart) as a function of cued position (Up -U, up-right –UR, right –R, down-right –DR, down –D, down-left –DL, left –L, upper-left –UL), color code: decoding performances. **C.** Decoding performance in time for correct (blue line, mean+/- s.e.m) and miss trials (red line, mean+/- s.e.m).

## *Spatial organization of spatial attention decoding errors*

In order to understand whether and how decoding errors organized spatially, we computed the confusion matrices for each cued condition, averaged over all subjects (Figure 3B). These confusion matrices quantify, for each cued position (portion of the pie chart), the probability with which the decoder associates brain activity to a given label, either matching

the cued location or not (smaller pie chart in each portion of the larger pie chart). These confusion matrices were computed using the decoding accuracy just prior to target presentation (see Figure 3A at T=0 sec), a time at which attention-related activity is expected to maximally account for upcoming target detection. Overall, these matrices show that covert attention decoding accuracy is always highest at the cued location (Figure 3B). Moreover, decoding errors are mainly associated with a confusion with locations neighboring the cued location (this is reproduced for Task 2, in supplementary figure S2B). This indicates that classification errors might either be due to noise in the signal or, most likely, reflect the fact that attention is intrinsically dynamic, as demonstrated using intra-cortical recordings approaches (Gaillard et al., 2020). This latter hypothesis predicts a correlation between decoding performance and behavioral performance. We thus compared decoding performance in time when training and testing was on correct trials (Figure 3C, blue line) or when training was on correct trials and testing was on missed trials in which subjects failed to detect the target (Figure 3C, red line). Compared to misses, correct trials showed highest decoding performances at time T=0 (last volume before target onset, Friedman test: $p<0.01$ and signed rank test: $p<0.05$) and 4.4 sec after target onset (visual response to the target, Friedman test $p<0.01$ and signed rank test: $p<0.01$). Overall, we thus demonstrate that decoding performance accounts for the subject's behavior and attention decoding accuracy is lower on miss trials as compared to correct trials. Taken together, these results indicate that our decoder reliably tracks how subjects implement spatial attention during individual trials.

### *Contribution of parietal and occipital voxels to attention decoding.*

Informative voxels as defined by the ANOVA are located both in the parietal and in the occipital cortex. In order to test whether both cortical regions equally contributed to attentional processes, we computed decoding performance in time using the voxels coming from either the parietal cortex, the occipital cortex or both (Figure 4A). To do so, we segmented the individual brains and we created occipital and parietal masks using FreeSurfer (Fischl, 2012), thus identifying the parietal and the occipital attention-related

voxels. The decoding performance when considering the occipital contributing voxels (Figure 4a, purple) is very similar to the decoding performance using the whole brain contributing voxels (figure 4a, pink), except right before target onset (T=0), where decoding performance was higher when considering all voxels irrespective of their cortical location. The parietal voxels decoding performance is consistently below the occipital voxels decoding performance although it remains well above chance level, with a decoding performance plateau at around 27%. The parietal decoding performance does not show any decoding peak at 4.4 sec following target onset, indicating that the target visual perception response is specific to occipital areas.

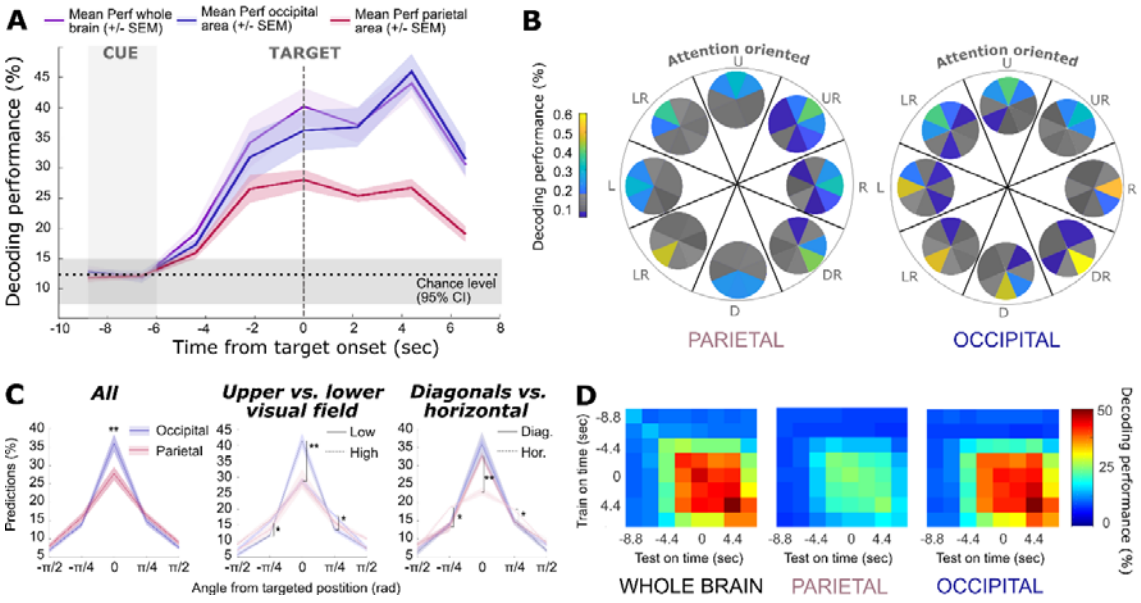


**Figure 4: Comparison of Parietal and Occipital SVM voxel based decoding of attention position. A.** Decoding performance in time centred on target onset based on parietal (red) or occipital (blue) or whole brain (purple) significant voxels (mean +/- s.e.m). **B.** Confusion matrices of parietal and occipital areas before target onset (all as in figure 3b). **C.** Percentage of confusion as a function of angle from cued position (0°). **D.** Decoding stability in time as a function of brain region.

In order to better characterize attention coding differences between the occipital and the parietal cortex with this real-time approach, we analyzed the confusion matrices (at time T=0 sec) when decoding from either the parietal or the occipital contributing voxels (Figure 4B left and right panels respectively). The same trend as described previously was observed, namely that the cued position is decoded with the highest performance and that decoding errors are highest closest to the cued location. Notably, the higher decoding performance

364 locations differed between the two brain regions. Figure 4C shows the decoding
365 performance per cued position, per brain region and the proportion of confusion as a
366 function of the distance between the decoded position and the actual cued position. As
367 already described in figure 4A (Figure 4C, left panel), occipital decoding performance is
368 higher than parietal decoding performance. This effect is specifically driven by the fact that
369 occipital decoding performance is higher for lower relative to upper visual field positions
370 (figure 4C, middle panel, Friedman test $p<0.01$, $p<0.01$ for the targeted position, $p<0.05$ for
371 the direct neighbors, blue stars). Complementing this effect, for higher visual field positions,
372 errors are more spread than for lower visual field positions (Figure 4C, middle panel, $p<0.05$
373 for -pi/4 neighbor and +pi/4 neighbors, signed rank test, blue stars). While this asymmetry in
374 the deployment of spatial attention has already been described by behavioral studies
375 (Carrasco et al., 2004; Ibos et al., 2009; Montaser-Kouhsari and Carrasco, 2009; Zénon et
376 al., 2009a), this is the first time this is captured at the single trial level. This spatial bias does
377 not exist in parietal regions. In contrast, in this region, a decoding performance bias in favor
378 of diagonal cued locations (i.e. away from the horizontal and vertical meridians) can be seen
379 with a more restricted spread of the errors to their nearest neighbors as compared to
380 meridians (Figure 4C, right panel, Friedman test $p<0.01$, Signed ranks test, $p<0.01$ for the
381 targeted position, $p<0.05$ for the direct neighbors, pinks stars). No such difference can be
382 seen between meridians and diagonals for the occipital region.

383 ***Within trial decoding stability.***

384 The above described observations correspond to a snapshot of attentional processes at
385 target presentation time. It is however evident from Figure 3A and 4A that attention-related
386 information builds up with time during the cue to target interval. An important question in this
387 respect is whether the attention-related code and recruited network are stationary during the
388 cue to target interval or not. To investigate within trial decoding stability in time, we trained
389 decoders on different times from 8.8 before to 4.4 seconds after target onset, and we
390 successively tested each decoder on these successive time bins, thus producing a cross-
391 temporal decoding map (Figure 4D, left: whole brain; middle: parietal; right: occipital). Whole

brain and occipital cross-temporal decoding maps are very similar, distinguishing a first stable coding epoch of attention orientation (from 4.4 secs before to 4.4 secs after target onset) and a second later epoch corresponding to target perception (from 4.4 sec to 6.6 sec after target onset). The parietal cross-temporal decoding map identifies a unique epoch of stable coding from 4.4 sec before up to 4.4 sec after target onset. This indicates that both attention and perception related processes can be captured in real-time from fMRI signal and that the codes and specific networks underlying these processes are only partially overlapping. In addition, these observations indicate that the codes and networks subserving either attention or perception are stable in time.

## *Within trial attentional spotlight location variability*

While average cross-temporal decoding is stable in time, as described in the previous section, recent behavioral -for review,(Gaillard and Ben Hamed, 2020)- and electrophysiological accounts (Gaillard et al., 2020) indicate that spatial attention is not a stationary process but varies rhythmically in time. In order to assess the degree of within trial-stability of spatial attention signals, we computed the proportion of trials for which the decoded position of attention matched cue instruction and for which the decoded position of attention was the same at target presentation and at previous time points. To do so, we selected those trials for which decoded attention at target presentation time matched the cued location. We then computed the percentage of angular confusion (relative to the cued position (0°), at time 2.2 and 4.4 seconds before target onset (supplementary figure S3). We show that in fMRI data, similarly to what has been reported in the prefrontal cortex of the macaque (Gaillard et al., 2020), attentional information is dynamic and classification improves as probability of target presentation increases. Specifically, on trials that end-up correctly classified at target presentation, 56% of them are correctly classified in the previous brain volume and only 24% of them are correctly classified in the brain volume before. Thus, in spite of the low temporal resolution of fMRI signals, fMRI-based decoding of attention allows to capture the dynamic nature of attention as reported both behaviorally and electrophysiological measures of higher temporal resolution.

## *Cortical topography of attentional processes*

In order to better characterize the relationship between the decoder and the visual and attentional brain organization, we identified for each attention selective voxel its preferred coding position and color coded this information on brain flat maps (Figure 5A). To do so, we performed a t-test with FDR correction on decoding voxels, for each position, against its fixation activity. For each position, only the significant voxels were considered ($p<0.05$, FDR corrected). This procedure was performed on the eight cued positions of the task, on cued positions grouped per quadrants, or on cued positions grouped per hemifield. Figure 5A shows the results for one subject. When analyzing as a function of cued hemifield, a clear contralateral activation in the occipital and parietal cortex can be seen. When analyzing as a function of cued quadrant or eight cued positions, only in the occipital cortex can we distinguish a clear topographical organization of voxel selectivity, matching occipital cortex topographical visual organization (Huang and Sereno, 2013; Wang et al., 2016). No such organization can be seen for the parietal cortex. This pattern is reproduced across all subjects. For example, a significant larger contralateral activation (as assessed by % activated voxels) can be observed compared to ipsilateral activation for parietal and occipital regions (Figure 5B, Friedman $p<0.001$, signed-rank for parietal $p< 0.001$, signed-rank for occipital, $p<0.001$). Importantly, a strong correlation was observed between the number of selective voxels and decoding performance when considering parietal voxels (Spearman, $Rho=0.9$, $p<0.01$). A trend towards this was also observed in the occipital cortex (Spearman, $Rho=0.7$, $p<0.054$). This indicates a link between the strength of the attentional information available for decoding during attention orientation and parietal attention-related control signals. These observations are reproduced in a second version of the attentional task with a different spatial configuration (4 orientations, 2 eccentricities, rather than 8 orientations and 1 eccentricity, Figure 5D). Taken together, these results confirm that spatial covert attention is associated with a topographically organized functional gating of BOLD activations by spatial attention orientation in the visual cortex. Most importantly, this demonstrates that this

information can be precisely recovered at the single trial level, at the time resolution of fMRI TR.

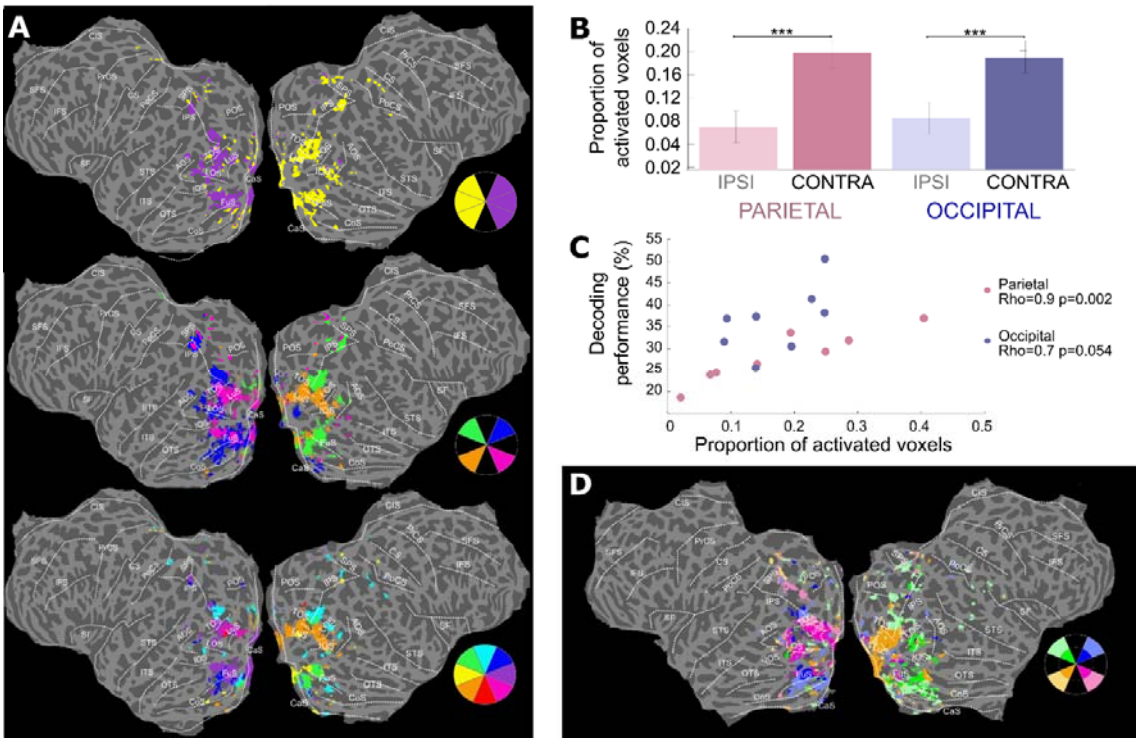


**Figure 5: Topographical organization of attentional decoding voxels**. **A.** Topography of voxels used for decoding (single subject). **B.** Proportion of selected voxels per brain region and per position (ipsilateral and contralateral), data represented as mean +/- s.e.m, Ranksum test across all subjects (***, p<0.001). **C.** Decoding performance as a function of contralateral hemisphere activation per position, Spearman correlation. **D.** Topography of voxels used for decoding during the 4 orientations and 2 eccentricities task (Task 2 of Figure 1, single subject, same as in A).

## *Decoding stability across scanning blocks and sessions*

In the perspective of applying single trial access to spatial decoding for neurofeedback protocols run on sessions independent from those on which the decoder was estimated, an important question is that of the reliability of our decoding across blocks and sessions. We thus first assessed reliability as a function of the number of blocks used for training (training on N blocks, testing on the remaining blocks, at time T=0, just before target onset – Figure 6A). Most of the subjects reach a decoding plateau after 10 blocks, i.e. two sessions on average (Figure 6A, red line). After that, the decoding performance does not necessarily increase with additional training blocks. This plateau ceils at around 50% of decoding accuracy. This can reflect a methodological limit in accessing to spatial attention from BOLD

fMRI signals. Alternatively, this reflects the intrinsic difficulty of subjects to sustain a precise attentional orientation in this task, as reflected by the spatial organization embedded in our confusion matrices (Figures 3B and 4B), the within trial decoding variability described in the previous section (supplementary figure S3) as well as recent behavioral (Gaillard and Ben Hamed, 2020) and electrophysiological accounts on rhythmic attention (Gaillard et al., 2020).

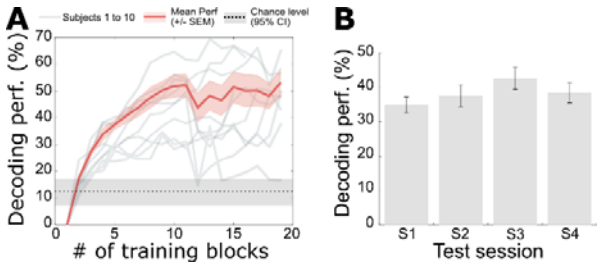


**Figure 6: Voxel activation-based decoding of attentional position is reliable across subjects and sessions. A.** Decoding performance before target onset as a function of the number of blocks used for training, grey line, individual subjects decoding performances across blocks, red line, mean +/- s.e.m). **B.** Decoding performance before target onset, while training on all except one session and testing on the remaining session (mean +/- s.e.m).

We then tested the stability of decoding across sessions (training on N-1 sessions, testing on the remaining session -Figure 6B). We show that decoding performance remains stable across sessions (no significant difference, Wilcoxon test p=0.3), even though these sessions have been recorded on different days (ranging from intervals of 1 day to 1 week). Given that we are able to perform real time fMRI preprocessing in less than 1 second per volume with the FRIEND toolbox (Basilio et al., 2015) (TR at 2.2sec), this thus opens the possibility of accumulating trials from different days to get a reliable decoder and developing covert attention-based neurofeedback protocols.

## Discussion

Contrary to sensory or motor cognition, decoding covert cognitive states at high temporal resolution is still challenging due to the fact that precise informational cognitive content can only be inferred by overt behavior and cannot be probed directly. This is rendered even more challenging due the fact that covert cognitive functions have recently been shown to be non-stationary and may vary rhythmically in time -for review,(Gaillard et al., 2020; Gaillard and

Ben Hamed, 2020)-. In the present study we achieve real-time single trial decoding of spatial attention orientation from non-invasive fMRI BOLD signals. In the following, we compare our results to prior literature and we discuss how decoding of spatial attention at the single trial level both reveals a refined understanding of how brain functions account for behavior (Loriette et al., 2021) and hold strong potential for the development of neurofeedback closed-loop applications (Loriette and Ziane, 2021).

### *Improved spatial resolution of single trial attention decoding relative to state of the art*

In this study, we show that it is possible to infer to locus of covert attention on a single trial basis using fMRI with a decoding accuracy significantly above chance level (12.5%), when classifying spatial attention in eight different locations. Mean accuracy reaches 40% across participants, but can reach up to 58% in some subjects. Prior fMRI studies only achieve a four-class single trial classification of attention to one of the four visual quadrants (chance at 25%) (Andersson et al., 2012; Ekanayake et al., 2018), albite with a higher reported average decoding accuracy (80%). In addition, relative to previous studies, the present study has several methodological strengths. A real-time monitoring of eye movements is achieved, interrupting trials in which subjects make eye movements, and thus preventing signal contamination by saccadic information or saccadic visual after effects. In addition, the task uses central low contrast cues thus preventing attentional signal contamination by visual cueing information. Overall, this is a major advance in the field as covert attention decoding has never been performed with this level of spatial precision with non-invasive approaches.

It is worth noting that although we report an average decoding performance for an eight-class classification of spatial attention, individual subject performance varied between 28 and 58%, indicating a large inter-individual variability. Decoding accuracy correlated with the proportion of parietal (and to a lesser extent occipital) voxels that were selected during the feature selection step, but not with overt behavioral performance ($R=0.11$, $p=0.64$). In other words, decoding accuracy correlated with the number of brain voxels that showed a specificity for one of the cued locations, i.e. with how spatial attention was topographically

implemented in each subject, irrespective of behavioral accuracy. This criterion might serve as an objective measure to identify subjects best suited for real-time decoding of their attentional function -e.g. for neurofeedback closed-loop applications.

## *Decoding reveals the dynamic feature of the attentional function*

Behavioral performance of subjects is predictive of spatial attention decoding performance. In fact, decoding is lower when performed on incorrect trials (in which subjects missed the target) as compared to when decoding is performed on correct trials. This is thus in agreement with what has already been reported in non-human primate invasive real-time access to spatial attention studies, whereby decoding accuracy is higher on correct than on missed trials (Astrand et al., 2016, 2015; De Sousa et al., 2021). Overall, decoding thus shows that attention-related information is less accurate on missed trials than on correct trials, accounting for behavioral failure.

Invasive animal studies actually demonstrate that the precise spatial locus of attention also varies, on correct trials, just prior to target presentation, such that on some trials, attention is decoded close to the expected location of the target, while on others, attention is decoded far away (Astrand et al., 2016, 2015; De Sousa et al., 2021). While it can be tempting to consider this as noise in the signal, these studies show that the closer the decoded attentional spotlight to expected target location, the higher the probability of detecting the trial, thus indicating that rather than reflecting noise in the signal, this variability in the locus of the attentional spotlight reflects noise in the attentional function itself. Accordingly, training a classifier on trials for which attention was initially decoded closest to expected target position enhances the correlation between decoding accuracy and behavior (De Sousa et al., 2021). In addition, tracking the attentional spotlight at a high temporal resolution reveals that it is not stable but rather, it moves around at a frequency of 8 to 12 Hz (Gaillard et al., 2021). Extending these observations to the current non-invasive decoding of attention, we would like to suggest that the specific structure of the confusion matrices described in figures 3B and 4B, does not reflect decoding performance on noisy signal. Rather, it captures the dynamic nature of spatial attention, such that subjects, while trying hard to focus their

attentional spotlight at the cued location cannot prevent it to explore space at close by locations (Gaillard et al., 2021). All this taken together strongly suggests that due to the dynamic nature of spatial attention function, the quest for ever improved decoding accuracy is an unreachable Grail. Rather than seeking that goal, research should seek to characterize the behavioural source of variability in the single trial decoding (Amengual and Ben Hamed, 2021; Loriette et al., 2021).

### *Decoding reveals the cortical topography of attentional control and gating*

We show that the parietal and the occipital cortex have distinct contributions to overall decoding performance, such that while maximal decoding accuracy is achieved using voxels from both cortical regions, occipital voxels have a higher attention-related informational content than parietal voxels. This is probably due to the fact that the spatially resolved topographical organization of the occipital cortex allows for enhanced spatial discrimination than that achieved in the parietal cortex. As a result, there is no strong correlation between the number of informative voxels in the occipital cortex and occipital decoding accuracy, indicating that fewer voxels suffice for the decoding. In contrast, the larger the number of parietal informative voxels, the higher the parietal decoding performance. This suggests an inter-individual difference accounted for by the specific parietal spatial map implemented in each subject.

Feature selected voxels reveal the topographical organization of the occipital cortex albeit this feature selection is based on attention information rather than on visual information. This attentional occipital topographical organization of the visual cortex is very similar to the visual retinotopic occipital maps reported in fMRI studies (Arcaro et al., 2009; Warnking, 2002). This topographic organization of attentional top-down biasing signals in the visual cortex in the absence of visual information reveals attentional gating in the occipital cortex, as already demonstrated by others (Datta and DeYoe, 2009; Kastner et al., 1998; Tootell et al., 1998; Ungerleider, 2000). This spatially resolved attentional gating thus supports the high-performance single trial decoding that we report here.

On top of this general attentional occipital gating, we show that occipital decoding accuracy is biased for low visual field compared to high visual field. This bias is consistent with previous behavioral work. Indeed, a very strong bias of visuospatial attention and visual perception toward the low visual field is described such that behavioral attentional performance is higher when implemented in the lower visual field (Carrasco et al., 2004; Montaser-Kouhsari and Carrasco, 2009; Zénon et al., 2009a). Our results suggest that the occipital decoding bias reported here most probably accounts for the behavioral biases reported in the literature, reflecting how efficiently attentional gating is implemented onto the occipital topographical map (Brefczynski and DeYoe, 1999; Kastner et al., 1999; Tootell et al., 1998). In addition to this upper vs lower visual field bias, we also describe an enhanced parietal decoding performance along the diagonals as compared to the horizontal and vertical meridians. Behavioral studies describe a performance bias in favor of the horizontal meridian compared to the vertical meridian and to the diagonals (Carrasco and Yeshurun, 2009; Corbett and Carrasco, 2011; Zénon et al., 2008; Zénon et al., 2009b, 2009a). It is thus unclear how the decoding bias reported here relates to the behavioral biases in previous studies. The decoding bias might actually reflect the topographical organization of attentional information in the parietal cortex, impacting its accessibility through decoding, rather than a functional bias. This will have to be confirmed experimentally.

### *Real-time decoding of spatial attention for neurofeedback closed-loop applications*

Importantly, we show that this single trial access to spatial attention is stable not only across blocks within the same session but also across sessions that are several days apart. In addition, we show that decoding ceils after only two sessions. Overall, this thus opens wide opportunities in term of fMRI-based attentional training, neurofeedback and closed-loop experimental designs (Weiskopf, 2012). Indeed, as the decoding is remarkably stable across sessions, we can ask our participants to come one two sessions to form the decoder and detect whether they are good candidates for real-time neurofeedback experiments (based on their overall decoding performance) and then come in several times and to perform fMRI-

based neurofeedback driven by this single trial decoding of attention. fMRI neurofeedback has already been achieved on cognitive functions such as categorical attention or confidence, and was associated with strong behavioral and functional effects (Cortese et al., 2017; deBettencourt et al., 2015; Loriette et al., 2021; Loriette and Ziane, 2021). While, until now, fMRI neurofeedback on higher order cognitive functions has been mainly performed on a binary basis (category 1 versus category 2 or focused/not focused), our work opens the way to perform a precise neurofeedback based on decoding the spatial position of attention in order to enhance or restore the attentional function. In the long term, this should allow attentional training in healthy participants, or perform attentional remediation for ADHD patient (attention brain deficit disorder) or brain damaged participants.

## Ethics declarations

The authors declare no competing interests.

## Acknowledgments

C.L., S.D.S. and SBH were supported by ERC BRAIN3.0 # 681978 and ANR-11-BSV4-0011 & ANR-14-ASTR-0011-01, LABEX CORTEX funding (ANR-11-LABX-0042) from the Université de Lyon, within the program Investissements d'Avenir (ANR-11-IDEX-0007) operated by the French National Research Agency (ANR) to SBH. C.L. was supported by a PhD funding from the French Ministry of Research and higher Education. S.H.B and S.C. were supported by ANR-16-CE37-0009-01.

## Author contribution

Conceptualization, C.L. and S.B.H.; Data Acquisition, C.L. C.D.S.; Methodology, C.L., S.C. and S.B.H.; Investigation, C.L. and S.B.H.; Writing – Original Draft, C.L.; Writing – Review & Editing, C.L., C.D.S., S.C. and S.B.H.; Funding Acquisition, S.B.H.; Supervision, S.B.H.

# References

Abraham, A., Pedregosa, F., Eickenberg, M., Gervais, P., Mueller, A., Kossaifi, J., Gramfort, A., Thirion, B., Varoquaux, G., 2014. Machine learning for neuroimaging with scikit-learn. Front. Neuroinformatics 8, 14. https://doi.org/10.3389/fninf.2014.00014

Amengual, J.L., Ben Hamed, S., 2021. Revisiting Persistent Neuronal Activity During Covert Spatial Attention. Front. Neural Circuits 15. https://doi.org/10.3389/fncir.2021.679796

Andersson, P., Ramsey, N.F., Raemaekers, M., Viergever, M.A., Pluim, J.P.W., 2012. Real-time decoding of the direction of covert visuospatial attention. J. Neural Eng. 9, 045004. https://doi.org/10.1088/1741-2560/9/4/045004

Arcaro, M.J., McMains, S.A., Singer, B.D., Kastner, S., 2009. Retinotopic Organization of Human Ventral Visual Cortex. J. Neurosci. 29, 10638–10652. https://doi.org/10.1523/JNEUROSCI.2807-09.2009

Astrand, E., Ibos, G., Duhamel, J.-R., Ben Hamed, S., 2015. Differential Dynamics of Spatial Attention, Position, and Color Coding within the Parietofrontal Network. J. Neurosci. 35, 3174–3189. https://doi.org/10.1523/JNEUROSCI.2370-14.2015

Astrand, E., Wardak, C., Baraduc, P., Ben Hamed, S., 2016. Direct Two-Dimensional Access to the Spatial Location of Covert Attention in Macaque Prefrontal Cortex. Curr. Biol. 26, 1699–1704. https://doi.org/10.1016/j.cub.2016.04.054

Astrand, E., Wardak, C., Ben Hamed, S., 2020. Neuronal population correlates of target selection and distractor filtering. NeuroImage 209, 116517. https://doi.org/10.1016/j.neuroimage.2020.116517

Astrand, E., Wardak, C., Ben Hamed, S., 2014. Selective visual attention to drive cognitive brain machine interfaces: from concepts to neurofeedback and rehabilitation applications. Front. Syst. Neurosci. 8. https://doi.org/10.3389/fnsys.2014.00144

Basilio, R., Garrido, G.J., Sato, J.R., Hoefle, S., Melo, B.R.P., Pamplona, F.A., Zahn, R., Moll, J., 2015. FRIEND Engine Framework: a real time neurofeedback client-server system for neuroimaging studies. Front. Behav. Neurosci. 9. https://doi.org/10.3389/fnbeh.2015.00003

Bouton, C.E., Shaikhouni, A., Annetta, N.V., Bockbrader, M.A., Friedenberg, D.A., Nielson, D.M., Sharma, G., Sederberg, P.B., Glenn, B.C., Mysiw, W.J., Morgan, A.G., Deogaonkar, M., Rezai, A.R., 2016. Restoring cortical control of functional movement in a human with quadriplegia. Nature 533, 247–250. https://doi.org/10.1038/nature17435

Boynton, G.M., 2005. Attention and visual perception. Curr. Opin. Neurobiol. 15, 465–469. https://doi.org/10.1016/j.conb.2005.06.009

Brainard, D.H., 1997. The Psychophysics Toolbox. Spat. Vis. 10, 433–436.

Branco, M.P., Freudenburg, Z.V., Aarnoutse, E.J., Bleichner, M.G., Vansteensel, M.J., Ramsey, N.F., 2017. Decoding hand gestures from primary somatosensory cortex using high-density ECoG. NeuroImage 147, 130–142. https://doi.org/10.1016/j.neuroimage.2016.12.004

Brefczynski, J.A., DeYoe, E.A., 1999. A physiological correlate of the “spotlight” of visual attention. Nat. Neurosci. 2, 370–374. https://doi.org/10.1038/7280

Brown, E.N., Frank, L.M., Tang, D., Quirk, M.C., Wilson, M.A., 1998. A Statistical Paradigm for Neural Spike Train Decoding Applied to Position Prediction from Ensemble Firing Patterns of Rat Hippocampal Place Cells. J. Neurosci. 18, 7411–7425. https://doi.org/10.1523/JNEUROSCI.18-18-07411.1998

Carrasco, M., Marie Giordano, A., McElree, B., 2004. Temporal performance fields: visual and attentional factors. Vision Res., Visual Attention 44, 1351–1365. https://doi.org/10.1016/j.visres.2003.11.026

Carrasco, M., Yeshurun, Y., 2009. Covert attention effects on spatial resolution, in: Srinivasan, N. (Ed.), Progress in Brain Research, Attention. Elsevier, pp. 65–86. https://doi.org/10.1016/S0079-6123(09)17605-7

Corbett, J.E., Carrasco, M., 2011. Visual Performance Fields: Frames of Reference. PLoS ONE 6, e24470. https://doi.org/10.1371/journal.pone.0024470

678 Corbetta, M., Patel, G., Shulman, G.L., 2008. The Reorienting System of the Human Brain:
679 From Environment to Theory of Mind. Neuron 58, 306–324.
680 https://doi.org/10.1016/j.neuron.2008.04.017
681 Corbetta, M., Shulman, G.L., 2002. Control of goal-directed and stimulus-driven attention in
682 the brain. Nat. Rev. Neurosci. 3, 201–215. https://doi.org/10.1038/nrn755
683 Cortese, A., Amano, K., Koizumi, A., Lau, H., Kawato, M., 2017. Decoded fMRI
684 neurofeedback can induce bidirectional confidence changes within single
685 participants. NeuroImage 149, 323–337.
686 https://doi.org/10.1016/j.neuroimage.2017.01.069
687 Datta, R., DeYoe, E.A., 2009. I know where you are secretly attending! The topography of
688 human visual attention revealed with fMRI. Vision Res. 49, 1037–1044.
689 https://doi.org/10.1016/j.visres.2009.01.014
690 De Sousa, C., Gaillard, C., Di Bello, F., Ben Hadj Hassen, S., Ben Hamed, S., 2021.
691 Behavioral validation of novel high resolution attention decoding method from multi-
692 units & local field potentials. NeuroImage 231, 117853.
693 https://doi.org/10.1016/j.neuroimage.2021.117853
694 deBettencourt, M.T., Cohen, J.D., Lee, R.F., Norman, K.A., Turk-Browne, N.B., 2015.
695 Closed-loop training of attention with real-time brain imaging. Nat. Neurosci. 18, 470–
696 475. https://doi.org/10.1038/nn.3940
697 Di Bello, F., Ben Hadj Hassen, S., Astrand, E., Ben Hamed, S., 2021. Prefrontal Control of
698 Proactive and Reactive Mechanisms of Visual Suppression. Cereb. Cortex N. Y. N
699 1991 bhab378. https://doi.org/10.1093/cercor/bhab378
700 Ekanayake, J., Hutton, C., Ridgway, G., Scharnowski, F., Weiskopf, N., Rees, G., 2018.
701 Real-time decoding of covert attention in higher-order visual areas. Neuroimage 169,
702 462–472. https://doi.org/10.1016/j.neuroimage.2017.12.019
703 Fiebelkorn, I.C., Saalmann, Y.B., Kastner, S., 2013. Rhythmic sampling within and between
704 objects despite sustained attention at a cued location. Curr. Biol. CB 23, 2553–2558.
705 https://doi.org/10.1016/j.cub.2013.10.063
706 Fischl, B., 2012. FreeSurfer. NeuroImage 62, 774–781.
707 https://doi.org/10.1016/j.neuroimage.2012.01.021
708 Gaillard, C., Ben Hadj Hassen, S., Di Bello, F., Bihan-Poudec, Y., VanRullen, R., Ben
709 Hamed, S., 2020. Prefrontal attentional saccades explore space rhythmically. Nat.
710 Commun. 11. https://doi.org/10.1038/s41467-020-14649-7
711 Gaillard, C., Ben Hamed, S., 2020. The neural bases of spatial attention and perceptual
712 rhythms. Eur. J. Neurosci. https://doi.org/10.1111/ejn.15044
713 Gaillard, C., Sousa, C.D., Amengual, J., Loriette, C., Ziane, C., Hassen, S.B.H., Bello, F.D.,
714 Hamed, S.B., 2021. Attentional brain rhythms during prolonged cognitive activity.
715 bioRxiv 2021.05.26.445730. https://doi.org/10.1101/2021.05.26.445730
716 Glaser, J.I., Benjamin, A.S., Chowdhury, R.H., Perich, M.G., Miller, L.E., Kording, K.P.,
717 2020. Machine learning for neural decoding. eneuro ENEURO.0506-19.2020.
718 https://doi.org/10.1523/ENEURO.0506-19.2020
719 Grootswagers, T., Wardle, S.G., Carlson, T.A., 2017. Decoding Dynamic Brain Patterns from
720 Evoked Responses: A Tutorial on Multivariate Pattern Analysis Applied to Time
721 Series Neuroimaging Data. J. Cogn. Neurosci. 29, 677–697.
722 https://doi.org/10.1162/jocn_a_01068
723 Hatsopoulos, N., Joshi, J., O'Leary, J.G., 2004. Decoding continuous and discrete motor
724 behaviors using motor and premotor cortical ensembles. J. Neurophysiol. 92, 1165–
725 1174. https://doi.org/10.1152/jn.01245.2003
726 Huang, R.-S., Sereno, M.I., 2013. Bottom-up Retinotopic Organization Supports Top-down
727 Mental Imagery. Open Neuroimaging J. 7, 58–67.
728 https://doi.org/10.2174/1874440001307010058
729 Ibayashi, K., Kunii, N., Matsuo, T., Ishishita, Y., Shimada, S., Kawai, K., Saito, N., 2018.
730 Decoding Speech With Integrated Hybrid Signals Recorded From the Human Ventral
731 Motor Cortex. Front. Neurosci. 12, 221. https://doi.org/10.3389/fnins.2018.00221

Ibos, G., Duhamel, J.-R., Ben Hamed, S., 2013. A functional hierarchy within the parietofrontal network in stimulus selection and attention control. J. Neurosci. Off. J. Soc. Neurosci. 33, 8359–8369. https://doi.org/10.1523/JNEUROSCI.4058-12.2013

Ibos, G., Duhamel, J.-R., Hamed, S.B., 2009. The Spatial and Temporal Deployment of Voluntary Attention across the Visual Field. PLOS ONE 4, e6716. https://doi.org/10.1371/journal.pone.0006716

Jenkinson, M., Beckmann, C.F., Behrens, T.E.J., Woolrich, M.W., Smith, S.M., 2012. FSL. NeuroImage 62, 782–790. https://doi.org/10.1016/j.neuroimage.2011.09.015

Kamitani, Y., Tong, F., 2005. Decoding the visual and subjective contents of the human brain. Nat. Neurosci. 8, 679–685. https://doi.org/10.1038/nn1444

Kastner, S., De Weerd, P., Desimone, R., Ungerleider, L.G., 1998. Mechanisms of directed attention in the human extrastriate cortex as revealed by functional MRI. Science 282, 108–111. https://doi.org/10.1126/science.282.5386.108

Kastner, S., Pinsk, M.A., De Weerd, P., Desimone, R., Ungerleider, L.G., 1999. Increased activity in human visual cortex during directed attention in the absence of visual stimulation. Neuron 22, 751–761. https://doi.org/10.1016/s0896-6273(00)80734-5

Kleiner, M., Brainard, D., Pelli, D., Ingling, A., Murray, R., Broussard, C., 2007. What's new in psychtoolbox-3. Perception 36, 1–16.

Landau, A.N., Fries, P., 2012. Attention samples stimuli rhythmically. Curr. Biol. CB 22, 1000–1004. https://doi.org/10.1016/j.cub.2012.03.054

Li, X., Morgan, P.S., Ashburner, J., Smith, J., Rorden, C., 2016. The first step for neuroimaging data analysis: DICOM to NIfTI conversion. J. Neurosci. Methods 264, 47–56. https://doi.org/10.1016/j.jneumeth.2016.03.001

Loriette, C., Amengual, J., Ben Hamed, S., 2021. Beyond the BCI: Decoding brain activity as a tool to understand neuronal mechanisms subtending cognition and behaviour. submitted.

Loriette, C., Ziane, C., 2021. Neurofeedback for cognitive enhancement and intervention and brain plasticity.

Montaser-Kouhsari, L., Carrasco, M., 2009. Perceptual asymmetries are preserved in short-term memory tasks. Atten. Percept. Psychophys. 71, 1782–1792. https://doi.org/10.3758/APP.71.8.1782

Padmanaban, S., Baker, J., Greger, B., 2018. Feature Selection Methods for Robust Decoding of Finger Movements in a Non-human Primate. Front. Neurosci. 12, 22. https://doi.org/10.3389/fnins.2018.00022

Pelli, D.G., 1997. The VideoToolbox software for visual psychophysics: transforming numbers into movies. Spat. Vis. 10, 437–442.

Posner, M.I., 1980. Orienting of Attention. Q. J. Exp. Psychol. 32, 3–25. https://doi.org/10.1080/00335558008248231

Sato, J.R., Basilio, R., Paiva, F.F., Garrido, G.J., Bramati, I.E., Bado, P., Tovar-Moll, F., Zahn, R., Moll, J., 2013. Real-Time fMRI Pattern Decoding and Neurofeedback Using FRIEND: An FSL-Integrated BCI Toolbox. PLoS ONE 8. https://doi.org/10.1371/journal.pone.0081658

Schwarz, A., Ofner, P., Pereira, J., Sburlea, A.I., Müller-Putz, G.R., 2017. Decoding natural reach-and-grasp actions from human EEG. J. Neural Eng. 15, 016005. https://doi.org/10.1088/1741-2552/aa8911

Simpson, G.V., Weber, D.L., Dale, C.L., Pantazis, D., Bressler, S.L., Leahy, R.M., Luks, T.L., 2011. Dynamic Activation of Frontal, Parietal, and Sensory Regions Underlying Anticipatory Visual Spatial Attention. J. Neurosci. 31, 13880–13889. https://doi.org/10.1523/JNEUROSCI.1519-10.2011

Thiery, T., Lajnef, T., Jerbi, K., Arguin, M., Aubin, M., Jolicoeur, P., 2016. Decoding the Locus of Covert Visuospatial Attention from EEG Signals. PLOS ONE 11, e0160304. https://doi.org/10.1371/journal.pone.0160304

Tong, F., Pratte, M.S., 2012. Decoding patterns of human brain activity. Annu. Rev. Psychol. 63, 483–509. https://doi.org/10.1146/annurev-psych-120710-100412

786 Tootell, R.B.H., Hadjikhani, N., Hall, E.K., Marrett, S., Vanduffel, W., Vaughan, J.T., Dale,
787 A.M., 1998. The Retinotopy of Visual Spatial Attention. Neuron 21, 1409–1422.
788 https://doi.org/10.1016/S0896-6273(00)80659-5
789 Trachel, R.E., Clerc, M., Brochier, T.G., 2015. Decoding covert shifts of attention induced by
790 ambiguous visuospatial cues. Front. Hum. Neurosci. 09.
791 https://doi.org/10.3389/fnhum.2015.00358
792 Tremblay, S., Doucet, G., Pieper, F., Sachs, A., Martinez-Trujillo, J., 2015. Single-Trial
793 Decoding of Visual Attention from Local Field Potentials in the Primate Lateral
794 Prefrontal Cortex Is Frequency-Dependent. J. Neurosci. 35, 9038–9049.
795 https://doi.org/10.1523/JNEUROSCI.1041-15.2015
796 Ungerleider, S.K. and L.G., 2000. Mechanisms of Visual Attention in the Human Cortex.
797 Annu. Rev. Neurosci. 23, 315–341. https://doi.org/10.1146/annurev.neuro.23.1.315
798 Wang, B., Guo, J., Yan, T., Ohno, S., Kanazawa, S., Huang, Q., Wu, J., 2016. Neural
799 Responses to Central and Peripheral Objects in the Lateral Occipital Cortex. Front.
800 Hum. Neurosci. 10. https://doi.org/10.3389/fnhum.2016.00054
801 Warnking, J., 2002. fMRI Retinotopic Mapping—Step by Step. NeuroImage 17, 1665–1683.
802 https://doi.org/10.1006/nimg.2002.1304
803 Weiskopf, N., 2012. Real-time fMRI and its application to neurofeedback. NeuroImage, 20
804 YEARS OF fMRI20 YEARS OF fMRI 62, 682–692.
805 https://doi.org/10.1016/j.neuroimage.2011.10.009
806 Wen, H., Shi, J., Zhang, Y., Lu, K.-H., Cao, J., Liu, Z., 2018. Neural Encoding and Decoding
807 with Deep Learning for Dynamic Natural Vision. Cereb. Cortex N. Y. N 1991 28,
808 4136–4160. https://doi.org/10.1093/cercor/bhx268
809 Zénon, A., Ben Hamed, S., Duhamel, J.-R., Olivier, E., 2009a. Attentional guidance relies on
810 a winner-take-all mechanism. Vision Res. 49, 1522–1531.
811 https://doi.org/10.1016/j.visres.2009.03.010
812 Zenon, A., Ben Hamed, S., Duhamel, J.-R., Olivier, E., 2008. Spatial and temporal dynamics
813 of attentional guidance during inefficient visual search. PloS One 3, e2219.
814 https://doi.org/10.1371/journal.pone.0002219
815 Zénon, A., Hamed, S.B., Duhamel, J.-R., Olivier, E., 2009b. Visual search without attentional
816 displacement. J. Vis. 9. https://doi.org/10.1167/9.11.9
817

818

# Supplementary material

## *Supplementary note 1: whole brain attention-related brain activations*

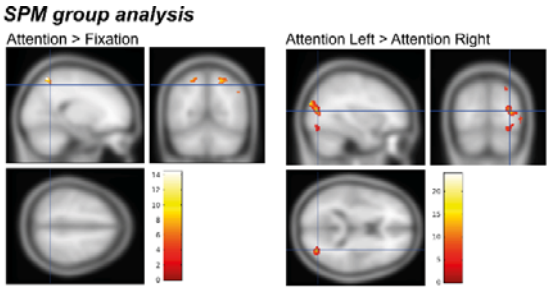


**Figure S1:** Contrast analysis reveals modulation of visual and parietal activity associated with spatial attentional orientation SPM group analysis; Left panel: Contrast between Attention and Fixation (FWE-corrected, p<0.05). Right panel: Contrast between Attention Left and Attention Right conditions.

In order to reproduce prior observations on whole brain spatial attention-related brain activation patterns at the group level, we contrasted Attention vs. Fixation conditions, where the Attention condition is sampled from 4secs following cue onset (in order to exclude potential cue evoked visual activations) up to target onset, and Fixation condition was sampled during the 10secs of fixation that the subjects had to perform every 5 trials (Figure S1). This spatially non-specific contrast revealed activations (p<0.01, non-corrected) in the right parietal area, which is reported to be involved in covert several spatial attention processes (Corbetta et al., 2008; Corbetta and Shulman, 2002). The Attention Left vs. Attention Right conditions contrast resulted in significant activations in the right occipital area (p<0.01, non-corrected, figure S1), i.e. an activation in visuals areas prior to target onset, illustrating an attentional gating, similarly to what has been reported by previous studies (Corbetta et al., 2008; Corbetta and Shulman, 2002; Simpson et al., 2011). The opposite contrast activated the left occipital cortex at mirror positions (data not shown). Taken together, this indicates that the task, in spite of its visual (low salience) and spatial (8 positions) characteristics, activated the expected covert spatial attention network. Activations do not reach FEW-corrected level due to the relatively small number of subjects as well as due to the fact that for the Attention Left vs. Attention right contrast, we are pooling, for each

condition, trials in which attention is oriented to three distinct spatial positions although all positions were oriented to the left or to the right.

## *Supplementary note 2: covert attention decoding performance in task 2*

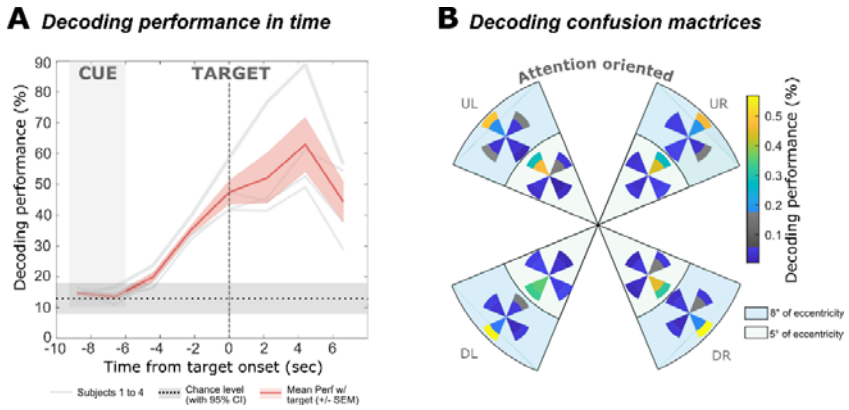


**Figure S2: Linear SVM decoder applied to selected feature modulated voxels allows access to attentional spotlight location with a high accuracy in the second task, in which the target can appear at four possible orientations and two possible eccentricities (5° and 8°). A.** Decoding performance in time on target present trials (red line, mean+/- s.e.m, gray lines: individual subjects). **B.** Confusion matrices per expected target position (smaller pie chart) as a function of cued position (up-right –UR, right –R, down-right –DR, down-left –DL, left –L, upper-left –UL), color code inside the small charts: decoding performances. Color code inside the bigger chart: eccentricity of the expected position.

The decoding performance and the evolution of decoding in time at the trial level for task 2 show a similar profile compared to what we found with task 1. In addition, while in task 1, confusions were spread across the direct neighbors of the cued position (in angle), the confusions for task 2 are more concentrated on the non-cued position with the same orientation but a different eccentricity. In other words, confusion is more marked along the eccentricity dimension than along the orientation dimension. Taken together, these results shown that the results obtained for both task are consistent, showing the reproducibility and thus, the strength of the results exposed in this article.

## *Supplementary figure 3: reliability of decoding in time*

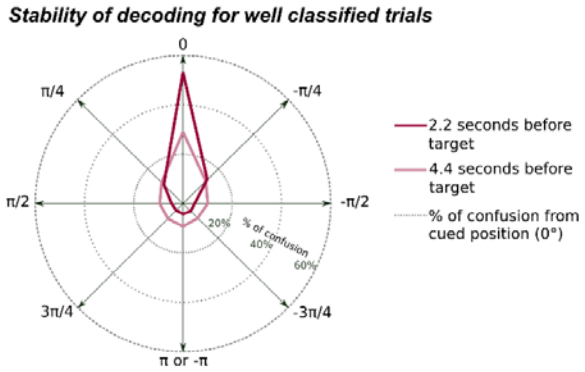


**Figure S3: Percentage of confusion relative to cued position 2.2 (dark red) and 4.4 seconds (pink) before target onset, for trials correctly classified at time 0 seconds from target onset.** For each correctly classified trial at target onset, we decode the position of attention one (2.2 seconds, dark red) and two volumes (4.4 seconds, lights red) before the target onset. This allows to investigate the stability of attention and decoding of each trial in time at the trial level.